

Research Paper

Combustion stage configurations for intercooled regenerative reheat gas turbine systems

G.B. Ariemma^a, G. Langella^{b,*}, P. Sabia^a, G. Sorrentino^a, M. de Joannon^a, R. Ragucci^a

^a Institute of Sciences and Technologies for Sustainable Energy and Mobility (STEMS-CNR), Naples, Italy

^b University of Naples Federico II, Naples, Italy

ARTICLE INFO

Keywords:

Brayton cycle
Combustion stage configurations
Global efficiency
MILD combustion

ABSTRACT

Low-power gas turbines have been widely used for decades as combined heat and power. In the recent years, they received increasing interest with respect to applications such as range extenders in the automotive sector and for alternative fuels use.

In this framework, the present work analyzes the combustion stages optimization of an intercooled regenerative reheat gas-turbine system, for a low power gas turbine. In particular, a thorough analysis was carried out to identify the optimal combustion system configuration in order to ensure suitable turbine inlet temperature and global efficiency of the thermodynamic cycle higher than 40%. Starting from the typical intercooled regenerative reheat gas turbine system, several configurations were analyzed. In particular, air bypass systems were introduced as suitable strategy able to tune the combustion chamber working temperatures and turbine inlet ones, according to operating requirements and combustion unit specifications. Furthermore, different bypass ratios were considered, analyzing the effectiveness of air bypass systems in terms of efficient combustion and reduced pollutant emissions (CO and NO_x).

An innovative cyclonic flow burner, assumed to operate under MILD (Moderate or Intense Low oxygen Dilution) combustion conditions, was considered as main combustion unit and in the reheat process. In this respect, the choice was motivated by the well-established high fuel flexibility and very low pollutants emission typical of such a combustion unit and the MILD process.

Analyses were performed considering methane as fuel, which is currently the most used fuel in land-based applications. However, results here reported have general validity and may be directly applied with respect to the use of innovative energy vectors.

1. Introduction

One of the driving challenges of the present century is the achievement of effective energy systems capable of satisfying the still growing energy demand while ensuring, in the long term, their sustainability. This imposes the simultaneous reduction of the use of fossil fuels and the increasing integration of renewable energy sources, in order to mitigate the global warming by reducing the CO₂ net emission in the atmosphere [1]. Along this road, the technological perspective focuses on boosting the use of renewable sources and alternative fuels [2–4], and increasing the efficiency of energy production systems [5].

In the case of gas turbines, the efficiency increase has been achieved by increasing the maximum temperature turbine inlet temperature (TIT). Consequences of this approach are the need of increasingly

sophisticated cooling techniques for the blades [6], the use of thermal barrier coatings [7] or special materials such as nickel-based super alloys [8]. However, more complex configurations and special materials imply higher costs. On the other hand, increasing operating temperatures entails increasing NO_x formation through thermal routes [9]. In this respect, systematic resort to lean and ultra-lean combustion conditions is often required to mitigate working temperature levels and, consequently, thermal NO_x formation [9]. However, lean and ultra-lean conditions may lead to the approach combustion instabilities and efficiency losses.

Unlike large-scale gas turbine plants, usually combined with steam plants, in medium and low power gas turbines systems the wide use of radial turbines instead of axial ones entails the not feasible implementation of blade cooling techniques. In this case a significant increase

* Corresponding author at: University of Naples Federico II, Department of Industrial Engineering, Via Claudio, 21, 80125 Naples, Italy.

E-mail address: giuseppe.langella@unina.it (G. Langella).

<https://doi.org/10.1016/j.applthermaleng.2024.122942>

Received 2 November 2023; Received in revised form 6 March 2024; Accepted 12 March 2024

Available online 13 March 2024

1359-4311/© 2024 The Author(s). Published by Elsevier Ltd. This is an open access article under the CC BY license (<http://creativecommons.org/licenses/by/4.0/>).

in the efficiency of the respective Brayton cycle can be achieved using several technological solutions as intercooling, reheating and regeneration [10–12]. Remarkably, all these techniques may be used simultaneously [13] and their coexistence allows for significant increases in efficiency, with moderate TIT values. Furthermore, several other strategies can be implemented in order to significantly increase the system efficiency. Among them, beneficial increase of the system efficiency can also be achieved with techniques such as humidification, already optimized for extended range vehicle applications of micro-gas turbines [14].

In these approaches, a micro gas turbine (mGT) is used, coupled with electric generators for recharging the batteries in automotive applications [15,16], thus realizing an ideally unlimited range extension (RE) of electric vehicles. In this respect, several studies are in progress on the optimization of the Brayton cycle of such turbo gensets [16–19]. A key point in such systems design is represented by the need of optimizing both the system configuration and operating parameters in order to ensure the attainment of the maximum efficiency at both the turbine stages and for the combustion process. This latter, in particular, is driven by the fundamental prerequisites of specific temperature levels, combustion stability and reduced pollutant emissions. Such a requirement poses some relevant issues related to the fact that the optimized operating conditions for combustion and turbine stages often do not match each other, even being antithetical in some specific cases.

In this framework, the present study focuses on the combustion stages optimization for a low-power, intercooled, reheated and regenerative gas turbine configuration, simultaneously ensuring high efficiency and moderate operating temperature levels for the expansion stages. To this aim, a bypass strategy of the only gas flows incoming in both the combustion chambers was proposed. In particular, the flow bypassing the combustion stage was supposed to recover heat from the combustion chamber and then mixed with the combustion products coming from the combustion chamber itself. The resulting stream was supposed then expanding in the turbine stages located downstream the combustion ones. In this respect, the effect of the bypass degree was analyzed, by verifying the required constraints in terms of global system efficiency, operating temperatures and pollutant emissions levels.

In particular, a cyclonic flow burner [20,21] operating under MILD combustion conditions [22,23] was considered as main combustion unit and in the reheat process. In this respect, despite conventional combustion regimes, MILD combustion allows to achieve uniform and stable combustion, with both moderate operating temperatures and reduced pollutant emissions. Indeed, under MILD conditions the high dilution and consequent local low oxygen levels prevents the stabilization of deflagrative/diffusive structures, while entailing an oxidation process mainly controlled by local mixture ignition mechanisms under moderate temperature and distributed over the whole combustion chamber volume [24,25]. Distributed ignition makes MILD combustion a highly fuel-flexible and resilient process. Indeed, the chemical evolution of the fuel oxidation is almost independent of the specific fuel type and operating conditions in terms of thermal load and fuel/air ratio [26]. Power plants and/or systems in which MILD combustion technology is used extend their operating range to a wide palette of different and innovative fuels (ammonia, hydrogen, etc.), overcoming the limitations usually hindering their utilization in conventional burners. In addition, the high resiliency of the oxidation process under MILD conditions allows to continuously adapt the thermal load to the specific demand, without compromising the combustion efficiency and the pollutant emissions [27].

The combustion process analysis was carried out considering methane as reference fuel. However, the adopted methodology show very general validity, thus being also relevant to the effective implementation of alternative fuels [28] or methane blending with hydrogen and ammonia [29,30].

The novelty of this work precisely lies in the bypass ratio optimization for the combustion stages of the considered mGT configuration,

implementing the MILD technology for the combustion process. This allows to provide useful insights with respect to feasible industrial applications of MILD combustion for mGT systems, for which the performance optimization is mainly achieved by humidification and hybridization techniques.

2. Methodology

An intercooled regenerative reheat gas turbine configuration devoted to the range extension of electric vehicles, equipped with a regenerator recovering heat on the outlet of the second turbine to pre-heat the incoming air stream fed to the first combustion system (reported in Fig. 1 along with the respective operating characteristics), was considered.

For the sake of simplicity, a single shaft configuration was considered, however the same analysis and combustion parameters optimization can be equally applied also to 2-shaft engines. In particular, this last option would allow compressor and turbine to operate at their respective optimal rotational speed.

For this reference system, an optimization procedure was performed, specifically focused on the combustion stages. This was carried out in order to identify the most effective configuration and optimal operating conditions ensuring stable combustion, acceptable pollutant emissions (namely CO and NO_x) and suitable operating temperatures (reported in red in Fig. 1), while meeting the operating requirements reported in Table 1 [16,17]. In particular, the optimization methodology was based on a parametric numerical analysis. Firstly, the most influent operating parameters for the analysed burners were identified, with respect to the reported requirements, afterwards the implementation of suitable solutions to ensure combustion stability, required temperatures levels and low pollutant emissions was analysed. In this respect, fundamental prerequisites driving the performed optimization analysis of the combustion stages were the turbine inlet temperature limit, fixed at 1370 K to be compatible with specific alloys of turbine elements for medium temperature applications [31], and the air mass flow rate equal to 6 kg/h for each kW of thermal power (kWt), essential to ensure a global efficiency higher than 40%. From these operating requirements, a recursive procedure was applied, in order to determine the optimal setup of the identified strategy to meet the needed targets.

A cyclonic-flow burner, extensively described in literature [32,33] and operating under MILD combustion conditions [22,23], was considered for both the combustion units of the configuration showed in Fig. 1. Such a choice is driven, to some extent, by the inlet flow requirements and turbine inlet temperature limit shown in Table 1 to reach a thermodynamic cycle global efficiency higher than 40%. Since, at the indicated flow conditions, the reactant mixture falls outside the flammability limits of the reference fuel in air (actual %CH₄ = 1.07 vol, LFL_{CH₄} = 4.4 % vol [34]), a combustion process not relying on a deflagrative structure stabilization but on distributed ignition [22], like the MILD combustion, is much more suited.

In this respect, MILD combustion process ensures wide range of combustion stability, moderate operating temperatures, flexibility to the fuel type and reduced pollutants formation [20,32].

With reference to the cyclonic burner, briefly it consists in $2 \cdot 10^{-3} \text{ m}^3$ prismatic chamber, with two anti-symmetrical couples of inlet tubes for oxidizer and fuel, orthogonally placed with respect to the outflow section, located in the reactor bottom face center. Such a configuration allows to establish a cyclonic flow in which the intense internal recirculation of combustion products induced by the centripetal motion covers a prominent role to attain a stable MILD conditions, without the use of complex external recirculation systems or elaborate injection strategies.

Starting from the reference configuration reported in Fig. 1, the combustion performance of both the burners of the gas turbine system were numerically evaluated. Then, ignition and oxidation times were analyzed with reference to the operating requirements reported in

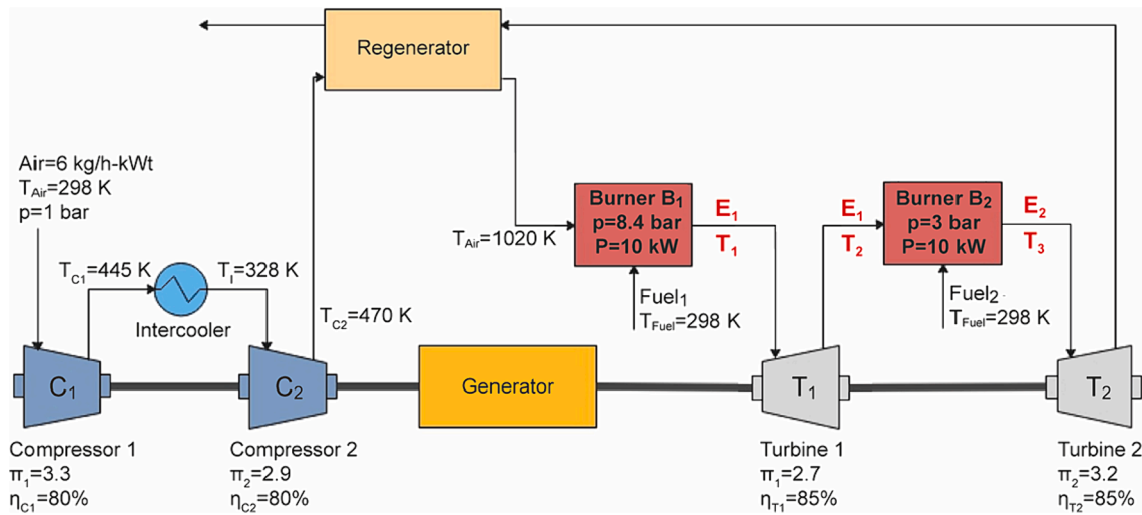


Fig. 1. Intercooled Regenerative Reheat gas turbine system configuration to be optimized.

Table 1

Operating requirements, burners and Brayton cycle specifics.

Turbine inlet temperature limit, K	1370	Maximum cycle pressure, bar	8.7
Air mass flow rate, kg/h-kWt	6	Compression ratio π_1	3.3
T_{in} Air Burner B ₁ , K	1020	Compression ratio π_2	2.9
Fuel	CH ₄	Expansion ratio η_1	2.7
Total thermal power, kWt	20	Expansion ratio η_2	3.2
T_{in} Fuel (T_0), K	298	Compression efficiency η_{C_i} , %	80
Single burner volume, m ³	$2 \cdot 10^{-3}$	Expansion efficiency η_{T_i} , %	85
Heat transfer coefficient, J/m ² -K-s	75.37	Required global efficiency η , %	>40

Table 1 in terms of inlet air temperatures, fuel and air flow rates, operating pressure and nominal residence times. Afterwards, air bypass systems were proposed as suitable strategies to optimize the combustion process in terms of stable combustion, low pollutant emissions and required turbine inlet temperatures. In particular, bypass strategies are already used in conventional burners for mGT, such as premixed (e.g. the AE-T100 kW), non-premixed (MTT Enertwin 3 kW) swirl stabilized flame or jet stabilized (e.g. DLR burners developed for these applications) systems. However, in the proposed analysis this strategy has been combined with cyclonic MILD combustors, thus coupling the benefits of both technologies.

The effectiveness of the proposed bypass strategies was investigated as a function of bypass number, location and intensity. In particular, for each proposed configuration, a two steps optimization procedure was carried out: first, the optimal bypass ratio was identified by analyzing the combustion performance for each burner in terms of operating temperature, combustion stability and pollutant formation minimization; then, energy balance for each component of the whole system configuration was performed, in order to verify the achievement of the required global system efficiency. Specifically, this latter was evaluated in agreement with Eq. (1):

$$\eta = \frac{(L_{T_1} + L_{T_2}) - (L_{C_1} + L_{C_2})}{Q_{th}} = \frac{L_{net}}{Q_{th}} \quad (1)$$

where L_T and L_C are the turbines power output and the compressors power input respectively, whose difference is equal to the system net power L_{net} while Q_{th} is the total thermal power input (20 kWt).

In detail, with respect to the combustion performance evaluation of both the burners reported in Fig. 1, these were modelled as Perfectly Stirred Reactors (PSR), provided by CHEMKIN PRO [35] package, with a volume of $2 \cdot 10^{-3}$ m³ and a nominal thermal power $P = 10$ kW each,

using methane as fuel and air as oxidant stream.

Numerical analyses were performed utilizing such a 0D approach since both the internal fluid dynamic configuration of the cyclonic burner and the key features of reactive structures associated with MILD combustion suggest a PSR behaviour. In this respect, the cyclonic flow field entails an intense and continuous mixing between recirculating combustion products and inlet fresh reactants, with very low mixing timescales compared with the characteristic chemical ones. This results in distributed reaction zone, involving the whole reactor volume, with almost uniform temperature and species distribution, thus emulating a PSR behaviour [36]. On the other hand, MILD combustion demonstrates nearly homogeneous characteristics at the macroscale [37], while at the microscale it shows reactive kernels evolving through both homogeneous [37] and diffusive structures [38]. In this respect, several numerical studies highlighted the importance of homogeneous processes (0D), especially for premixed feeding modes, wherein a PSR emerges as an appropriate reference paradigm [39].

Simulations were performed in both adiabatic and non-adiabatic conditions. Specifically, for this latter case the heat transfer coefficient was set equal to 75.37 J/m²-K-s, as estimated in a previous work [40], while a heat exchange area of 0.12 m² was imposed since characteristic of the considered burner [27,41]. The external ambient temperature for the heat exchange quantification was set as logarithmic mean difference between the inlet and outlet air bypass temperatures [42]. Furthermore, combustion stability and pollutant formation were investigated by using the C₁-C₃ detailed kinetic mechanism [43].

3. Results

3.1. Evaluation of the system combustion performance

Preliminary analyses were performed in order to numerically evaluate the combustion performance of both the burners of the gas turbine system, following the system configuration showed in Fig. 1. In particular, these were modeled as Perfectly Stirred Reactors (PSR), in adiabatic conditions, in order to analyze the possibility of stabilizing the oxidation process for the inlet conditions reported in Table 1.

As reported in Table 2 these conditions impose the burners working in extremely fuel-lean conditions, at equivalence ratio values equal to 0.103 and 0.115 respectively. In particular, with respect to Burner B₁, the air inlet temperature $T_{air} = 1020$ K ensures the reactive mixture ignition, although the combustion system shows very poor performance, as testified by the low operating temperature ($T_1 \sim 1220$ K) and very high CO emissions ($\sim 10^4$ ppm). On the other hand, the resulting inlet

Table 2

Computed operating conditions of Burner B₁ and Burner B₂ with reference to system configuration reported in Fig. 1.

Burner B ₁			Burner B ₂		
%CH ₄ ⁱⁿ , vol	1.07		%CH ₄ ⁱⁿ , vol	1.07	
%O ₂ ⁱⁿ , vol	20.77		%CO ₂ ⁱⁿ , vol	1.07	
%N ₂ ⁱⁿ , vol	77.15		%H ₂ O ⁱⁿ , vol	2.13	
%Ar ⁱⁿ , vol	1.00		%O ₂ ⁱⁿ , vol	18.43	
equivalence ratio	0.103		%N ₂ ⁱⁿ , vol	76.34	
T ₁ , K	1224		%Ar ⁱⁿ , vol	0.96	
T ₂ , K	987		equivalence ratio	0.115	
CO 15 %O ₂ , ppm	~10 ⁴		T ₃ , K	OUT	

conditions of Burner B₂ in terms of temperature (T₂ ~ 990 K) and mixture composition do not allow the oxidation process stabilization.

Therefore, in order to identify the main parameters to be optimized and, consequently, suitable strategies aiming at ensuring stable and effective combustion with low pollutant emissions and required turbine inlet temperatures, further focalized numerical analyses were performed.

In particular, ignition delay times τ_{ign} (time at which a temperature increase equal to 10 K with respect to the non-reactive conditions occurs), oxidation times τ_{ox} (time to achieve the stationary system temperature) and nominal residence times (ratio between the reactor volume and inlet volumetric flow rate) of a reactant mixture evolving under the conditions reported in Table 1 were analyzed and showed in Fig. 2, along with the computed CO emissions. Specifically, a parametric analysis was performed by varying the operating pressure and temperature in the range 1 bar < p < 15 bar and 950 K < T < 1100 K,

respectively, in order to cover a wide range of possible operating states. The ignition delay times were evaluated under batch conditions [35], while a PSR model was employed for the oxidation times evaluation [35], as reported in Section 2. For this latter, the air mass flow rate was set equal to 120 kg/h, as required for a total thermal power input equal to 20 kWt.

With respect to Fig. 2a, monotonic decreasing trends characterize τ_{ign} as a function of the operating pressure for all the investigated temperatures. In particular, ignition delay time decreases from 0.5 s down to 0.01 s at increasing T from 950 up to 1100 K, as expected. On the other hand, oxidation times τ_{ox} increase by increasing the operating pressure and ranges between 0.3 s and 2.2 s, as reported in Fig. 2b, with opposite trend with respect to τ_{ign} . Finally, the nominal residence time (grey area in Fig. 2b) always remains lower than 0.45 s for all the investigated pressure and temperature values. Specifically, this behavior entails a reactant mixture residence time lower than the characteristic one required to totally convert it to complete combustion products (τ_{ox}). Consequently, such a condition entails incompatible oxidation and nominal residence times, resulting in incomplete and essentially ineffective combustion process for the operating conditions of interest reported in Table 1. This results in significant emissions of partially oxidized species (CO). Indeed, as shown in Fig. 2c, CO levels in the exhausts are always ranged between 10³-10⁵ ppm, testifying the requirement for suitable improvements to increase the process performance.

3.2. Optimization of the system configuration: Burner B₁

Results analyzed in Section 3.1 highlighted the need of identifying suitable strategies ensuring the reactants ignition and their complete

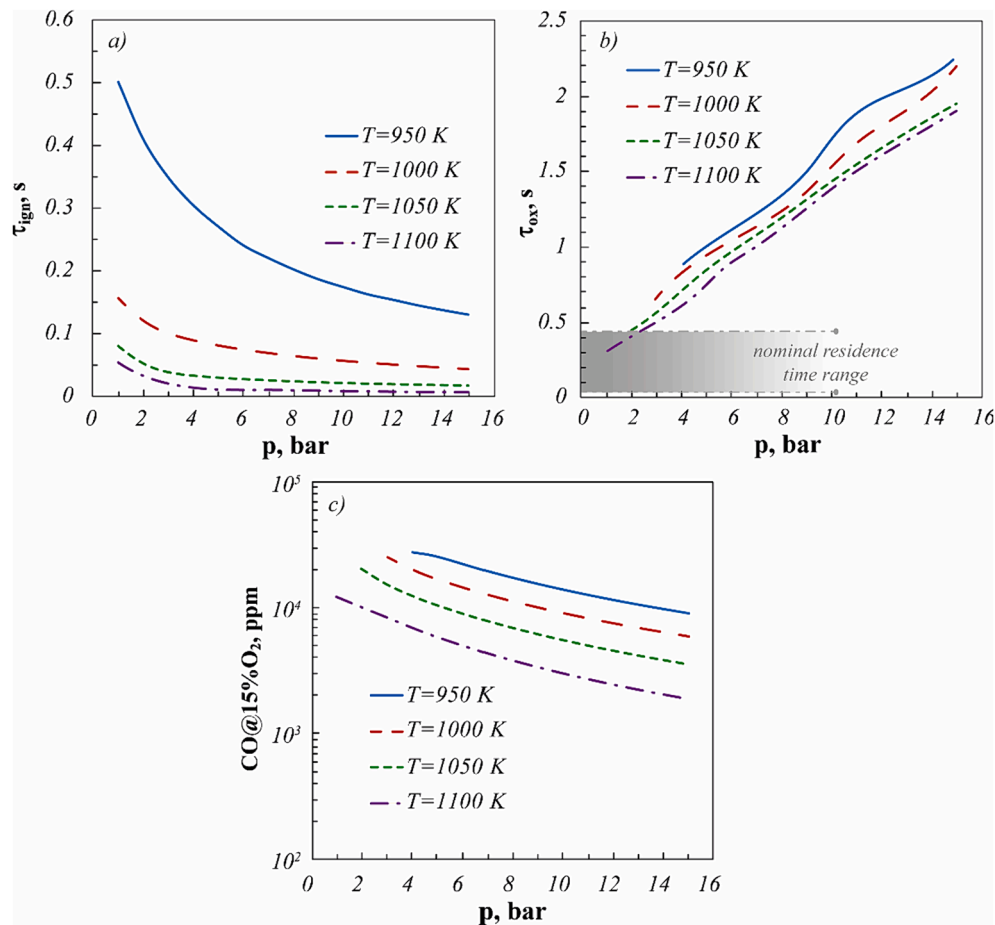


Fig. 2. (a) Ignition delay times (τ_{ign}), (b) oxidation time (τ_{ox}) and numerical CO emissions (c) as a function of operating pressure and temperature. CH₄. Reference conditions reported in Table 1.

and stable oxidation, while meeting the operating targets of Table 1. To this aim, it is essential to investigate useful configurations able to achieve compatible reactor residence times and reactants mixture oxidation ones. In this respect, among the possible effective strategies (i.e. larger reactor volumes, reduced thermal power etc.), the partition of the total air flow rate fed to the first reactor, coming from the regenerator system, was investigated. Such a solution was selected since it can beneficially affect the combustion process by increasing both the nominal residence times and the equivalence ratio values in the burner, as showed in Fig. 3, both essential to achieve stable combustion conditions. Specifically, air bypass ratio levels $\%R_1 = \frac{Air_2}{Air_1 + Air_2} \cdot 100$, on mass basis, were systematically investigated in the range $10 < \%R_1 < 90$, corresponding to equivalence ratio values of the Burner B₁ ranging between 0.1 and 1 and, consequently, nominal residence time between 0.2 and 1.6 s.

In this framework, the proposed system configuration was shown in Fig. 4. In particular, the air bypass stream was supposed to absorb the heat exchanged by the reactor and then mixed with the combustion product outgoing from the burner itself. In this respect, the heat exchange analysis between the bypass air and the burner external surface would need an in-depth and dedicated study, according to the design strategies adopted for bypass systems such as enveloping or passing through the combustion chamber. However, this is beyond the aim of presented paper, therefore the approach here proposed of using the bypass air to recover the burner exchanged heat is only conceptually analyzed since representing a simple and feasible configuration to meet the needed requirement in terms of global system efficiency.

In particular, the influence of air bypass ratio $\%R_1$ was analyzed by evaluating its impact on combustion stability, pollutant emissions and operating temperature levels of the Brayton system configuration.

In Fig. 5 operating temperatures and pollutant emission levels are reported as a function of the air bypass ratio $\%R_1$. With reference to Fig. 5a, by increasing $\%R_1$ the Burner B₁ temperature (T_1) monotonically increases. Such a result is expected, due to the resulting equivalence ratio increase with $\%R_1$, as showed in Fig. 3, that in turn ensures the oxidation process stabilization. In particular, T_1 ranges between 1200 and 1750 K for $R_1 = 10\%$ to $R_2 = 90\%$ respectively. The corresponding global heat exchange of the burner consequently varies between a minimum of 4% ($R_1 = 10\%$) up to 40% ($R_1 = 90\%$) of the total inlet thermal power level (considering both the fuel thermal input and the inlet air sensible enthalpy). This, in turn, results in air bypass

temperature profile (T_4) monotonically increasing from about 1100 K up to 1185 K as a function of $\%R_1$.

Similarly, the inlet gas temperature profile of Turbine T₁ (T_5) smoothly increases by increasing $\%R_1$. In particular, the Turbine T₁ inlet temperature ranges between 1190 and 1260 K for all the investigated $\%R_1$, approaching the Burner B₁ exit temperature (T_1) by decreasing the air bypass ratio, as expected. On the other hand, inlet temperature of Burner B₂ (T_2), corresponding to Turbine T₁ exit temperature, keeps almost constant and in the range 950–1000 K. These low temperature level affects the oxidation process effectiveness in the second combustion stage (B₂). Indeed, a very low temperature increase characterizes the gas flow outgoing from Burner B₂, as testified by the turbine inlet temperature T_3 in the range 970–1030 K.

Nevertheless, it is worth noting that the partition of the total air flow rate fed to the first reactor entails stable combustion and inlet temperatures for both the turbines of the investigated configuration always lower than the allowable limit of 1370 K, not exceeding 1260 K and 1030 K respectively.

With respect to pollutant emissions characterizing both the burners of the system configuration, NO_x and CO levels normalized at 15 %O₂ are reported in Fig. 5b as a function of $\%R_1$. Specifically, NO_x emissions always stay below 4 ppm, for all the investigated conditions, due to the moderate combustion operating temperatures. Instead, CO emissions show different behavior depending on the considered burner. In particular, a non-monotonic trend characterizes CO levels of Burner B₁, with a minimum of about 20 ppm located around $R_1 = 87\%$ (corresponding to an equivalence ratio equal to 0.8) and increasing CO emissions for both higher and lower $\%R_1$. Specifically, as previously shown in Fig. 3, $R_1 < 87\%$ entails the decrease of both the nominal residence times (<1s) within the reactor and inlet global equivalence ratio (<0.8), thus resulting in lower operating temperatures ($T_1 < 1700$ K, Fig. 5). This affects the combustion process performance by entailing a lower conversion of the inlet fuel to complete combustion products and, thus, increasing CO emissions. On the other hand, for $R_1 > 87\%$ the lower oxygen availability due to the inlet equivalence ratio increase entails increasing CO emissions, as reported in previous works [20]. Instead, CO levels of Burner B₂ always keep higher than about $7 \cdot 10^3$ ppm, independently of the investigated bypass ratio of the Burner B₁. This behavior can be ascribed to the very short residence times (<0.05 s) and low operative temperatures (<1050 K) characterizing the second combustion stage. These operating conditions entail incomplete fuel oxidation, similarly to what highlighted in Section 3.1 with respect to the Burner B₁ in the configuration without the air bypass system.

3.3. Optimization of the system configuration: Burner B₂

The analysis reported in Section 3.2 highlighted the effectiveness of the investigated air bypass strategy to optimize the operating conditions for the first burner of the considered gas turbine system configuration. Furthermore, it also pointed out the scarce combustion performance of the second combustion stage (Burner B₂).

In this respect, in order to attain effective combustion and allowable CO emission levels also for Burner B₂, an optimization strategy similar as though for the first combustion chamber of the gas turbine system was proposed. In this respect, the effectiveness of a further partition of the total inlet flow fed to the second reactor (Burner B₂) was investigated, as reported in the configuration of Fig. 6.

Specifically, the bypass ratio R_1 was set equal to 87%, identified as optimal operating condition for Burner B₁ in terms of operating temperatures, CO and NO_x emissions, while the bypass levels proposed for the second burner ($\%R_2 = \frac{D_2}{D_1 + D_2} \cdot 100$, on mass basis), were systematically investigated in the same range proposed for Burner B₁ ($10 < \%R_2 < 90$).

In this respect, in Fig. 7 operating temperatures, CO and NO_x emission levels for Burner B₂ as a function of the air bypass ratio $\%R_2$ are

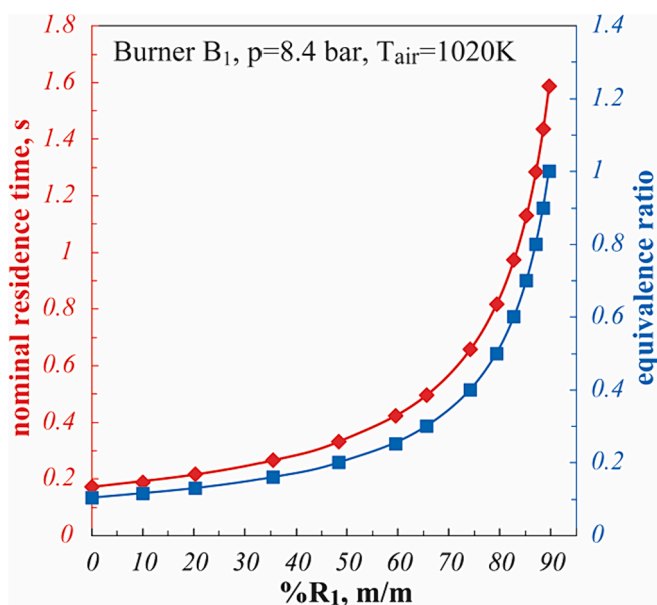


Fig. 3. Nominal residence time and equivalence ratio of Burner B₁ as a function of air bypass ratio R_1 . $T_{air} = 1020$ K, $p = 8.4$ bar.

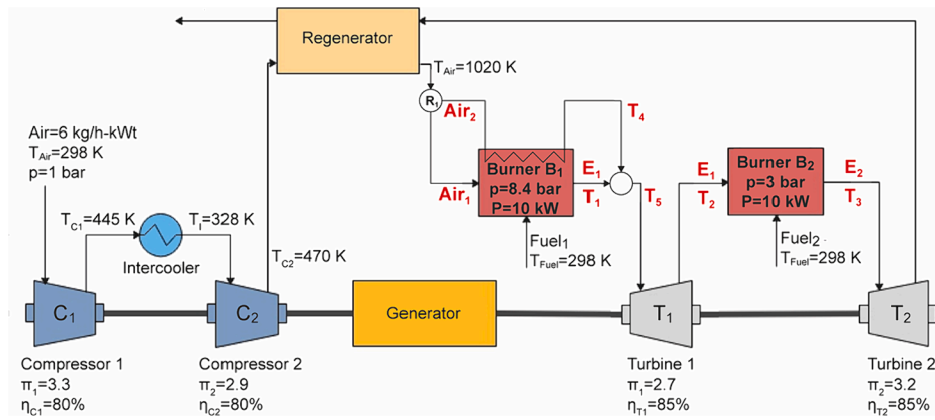


Fig. 4. Scheme 1: System configuration with Air bypass to Burner B₁.

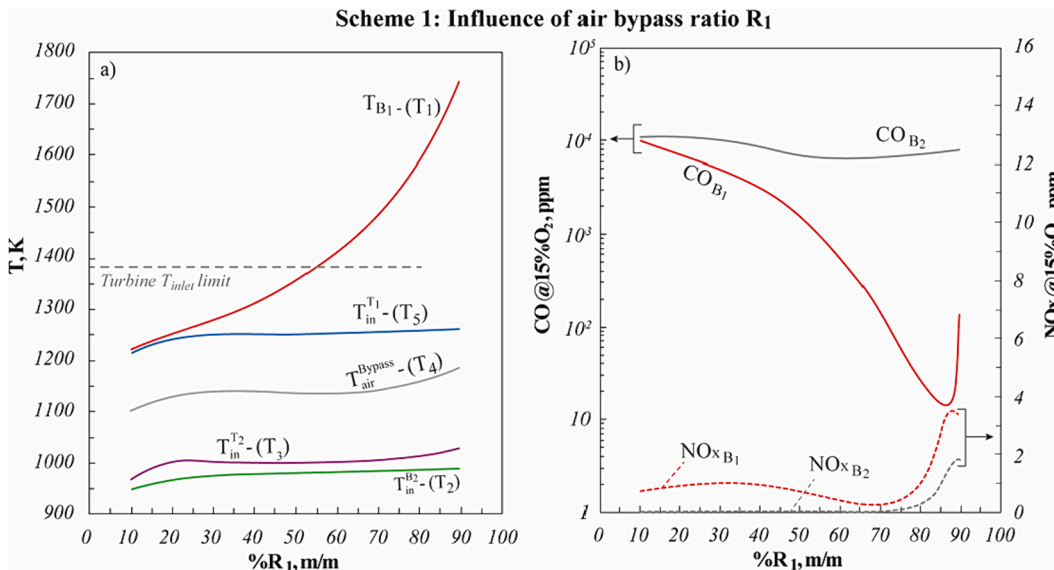


Fig. 5. Scheme 1: Operating temperatures (a), CO and NO_x emissions (b) as a function of the air bypass ratio of Burner B₁ (%R₁).

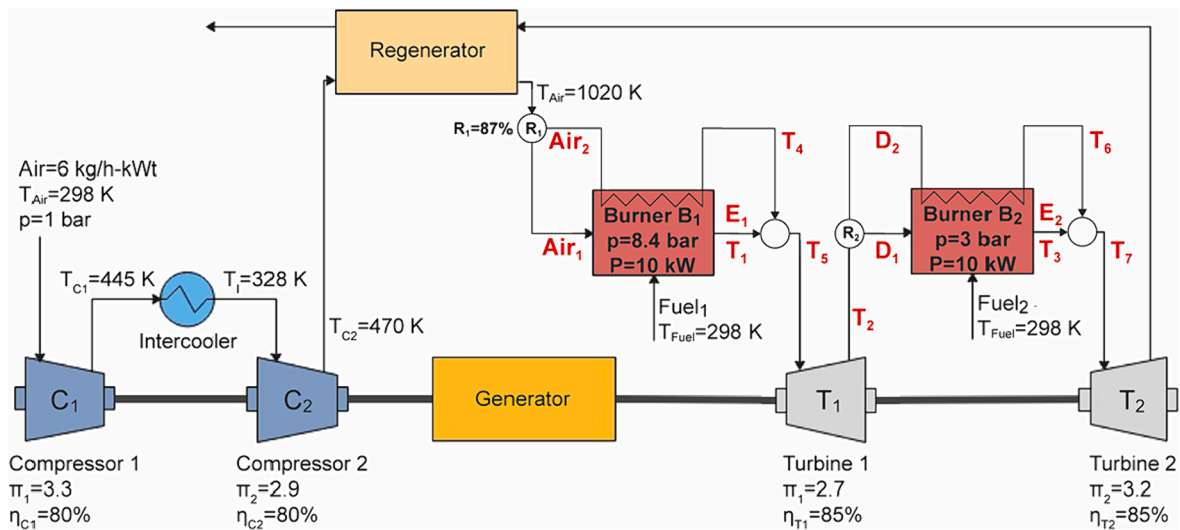


Fig. 6. Scheme 2: System configuration with bypass strategies for both the burners.

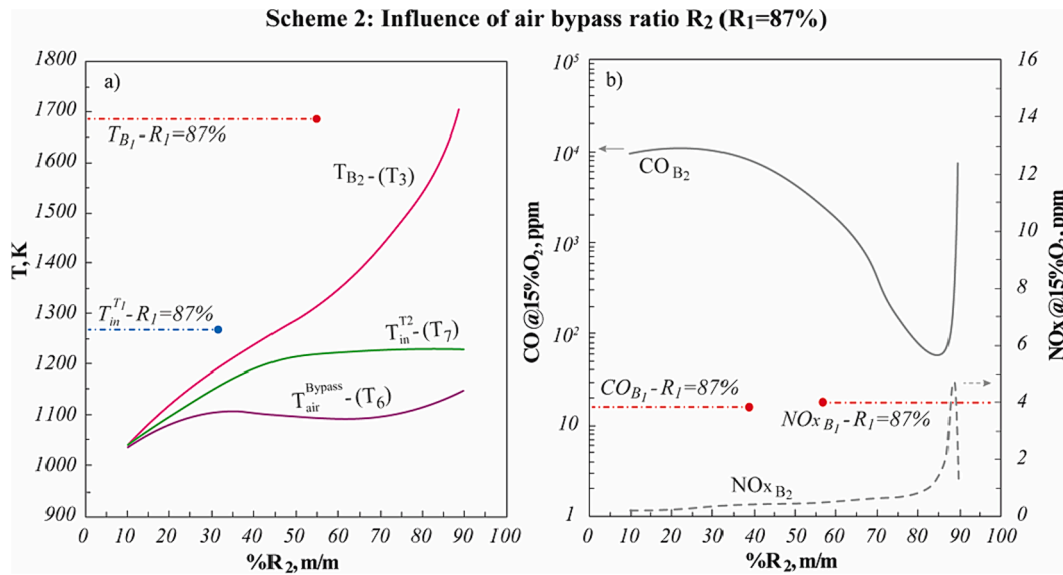


Fig. 7. Scheme 2: Operating temperatures (a), CO and NO_x emissions (b) as a function of the bypass ratio of Burner B₂ ($\%R_2$). $R_1 = 87\%$.

shown.

With reference to Fig. 7a, operating temperature levels show coherent profiles to those obtained for Burner B₁, with increasing trends by increasing $\%R_2$.

In particular, Burner B₂ operating temperature (T_3) increases from about 1040 K up to 1700 K, while air bypass temperature levels (T_6) are ranged between 1030 and 1150 K. The resulting turbine inlet temperatures also show a monotonic increasing trend and, in particular, they keep always lower than the maximum allowable limit of 1370 K. With respect to Fig. 7b, CO emission profile show a non-monotonic trend as a function of $\%R_2$, in agreement with the CO emission trend of Burner B₁ reported in Fig. 5b, with the minimum located at $R_2 = 85\%$. On the other hand, NO_x emissions keep very low in the whole investigated $\%R_2$ range, not exceeding 5 ppm.

Hence, as $R_1 = 87\%$ for Burner B₁, $R_2 = 85\%$ (corresponding to a global inlet equivalence ratio equal to 0.78) was identified as optimal bypass ratio value for Burner B₂. This is able to ensure effective and complete oxidation of the reactant mixture, with CO and NO_x emissions keep lower than 60 ppm and 2 ppm, respectively, and inlet temperature for Turbine T₂ of about 1220 K. Moreover, the identified optimal bypass ratios allow both the burner and the turbines of the system to operate in very similar conditions.

Finally, the achievement of the required global energy efficiency of the optimized Brayton system configuration with bypass strategies for both the burners was evaluated with respect to $\%R_2$ (Fig. 8), in agreement with Eq. (1). In this respect, for all the analyzed conditions in terms of $\%R_2$ the system global efficiency η keeps always higher than the minimum required target ($\eta > 40\%$), with an increasing trend by increasing $\%R_2$.

In particular, the considered intercooled regenerative reheat gas turbine system, with optimized combustion stages by bypass strategies ($R_1 = 87\%$ and $R_2 = 85\%$) ensures a global energy efficiency of about 49%, testifying the effectiveness of the investigated solutions also with respect to this target.

The gradual slight increase of global efficiency as a function of $\%R_2$ is correlated both to the increase of combustion efficiency (due to the reduction of CO) and to the slight increase in the inlet temperature of the second turbine. This last parameter increases the expansion work and therefore the network of the analyzed system, thus resulting in an increased system efficiency. Finally, starting from a higher turbine inlet temperature, the turbine outlet temperature is also increased, allowing greater heat recovery, with a further improving effect on the global

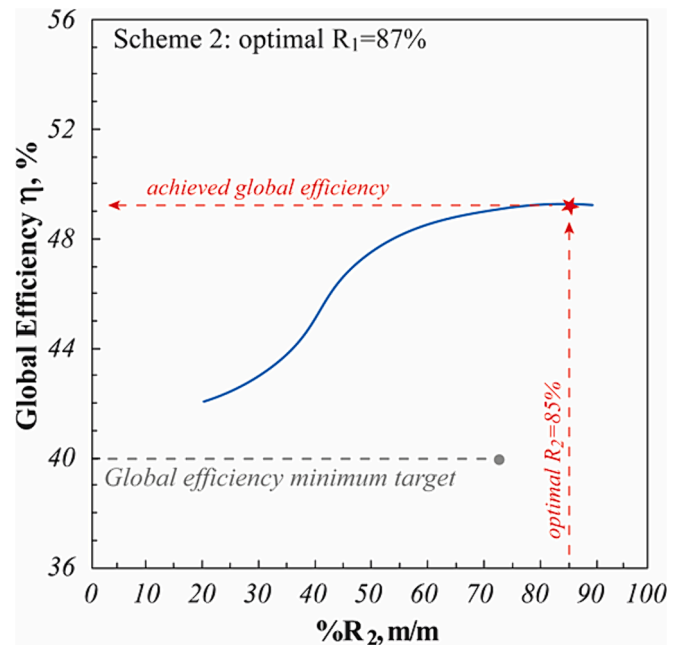


Fig. 8. Scheme 2: Global energy efficiency as a function of the bypass ratio of Burner B₂ ($\%R_2$). $\%R_1 = 87\%$.

energy efficiency.

4. Conclusions

In the present work the optimization of the combustion stages of a typical intercooled regenerative reheat gas turbine system was carried out, with specific focus on system operating temperatures, turbine inlet temperature levels and pollutant emissions (CO, NO_x). A cyclonic-flow combustion chamber operating under MILD combustion conditions was considered as innovative combustion unit implemented in the analyzed configuration, in order to meet the requirements of stable combustion, moderate operative temperatures and minimized pollutant formation. In particular, the best operating conditions for methane combustion have been outlined through the investigation of different system configurations.

The preliminary analysis performed to evaluate the combustion performance under the specifics reported in Table 1 highlighted the need of identifying useful strategies able to achieve compatible reactor residence times and reactants mixture oxidation ones. In this respect, the partition of the total inlet flow rate for each burner by bypass systems was proposed as suitable strategy to ensure both longer nominal residence times and higher equivalence ratio values for both the combustion stages.

In particular, the system configuration with bypass ratios equal to $R_1 = 87\%$ and $R_2 = 85\%$ was identified as optimal solution for the considered intercooled regenerative reheat gas turbine system, with turbine inlet temperatures lower than the imposed limit of 1370 K, CO and NO_x emissions lower than 60 ppm and 2 ppm respectively and a global energy efficiency of about 49%.

In this framework, the proposed analysis can represent a useful methodology to simply identify and assess suitable strategies to optimize the combustion stages of gas turbine thermodynamic configurations, especially for the use of unconventional energy carriers, such as low calorific (raw biofuel) and no-carbon fuels, for which the combustion process optimization still represents the main issue.

CRedit authorship contribution statement

G.B. Ariemma: Conceptualization, Data curation, Investigation, Methodology. **G. Langella:** P. **Sabia:** Conceptualization, Investigation, Supervision. **G. Sorrentino:** M. **de Joannon:** Conceptualization, Supervision. **R. Ragucci:** Conceptualization, Supervision, Writing – review & editing.

Declaration of competing interest

The authors declare that they have no known competing financial interests or personal relationships that could have appeared to influence the work reported in this paper.

Data availability

No data was used for the research described in the article.

Acknowledgments

This research was partly funded by the European Union in the framework of NextGeneration EU initiatives under the following initiatives of the National Recovery and Resilience Plan (NRRP-PNRR):

- “POR H2 AdP MMES/ENEA-CNR”, Mission 2, Component 2, Investment 3.5 “Ricerca e sviluppo sull'idrogeno”, CUP: B93C22000630006;
- “Centro Nazionale Mobilità Sostenibile (CNMS-MOST)”, Mission 4, Component 2, Investment 1.4, CUP: B43C22000400001;
- “Network 4 Energy Sustainable Transition – NEST” - Mission 4, Component 2, Investment 1.3, CUP: B53C22004060006.

References

- [1] R. Newell, D. Raimi, S. Villanueva, B. Prest, Global Energy Outlook 2021: Pathways from Paris, 2021.
- [2] S. Sangeeta, M. Moka, M. Pande, R. Rani, M. Gakhar, J. Sharma, A.N. Rani Bhaskarwar, Alternative fuels: an overview of current trends and scope for future, Renew. Sust. Energy Rev. 32 (2014) 697–712, <https://doi.org/10.1016/j.rser.2014.01.023>.
- [3] E. Mokrzycki, A. Uliasz-Bocheńczyk, Alternative fuels for the cement industry, Appl. Energy 74 (2003) 95–100, [https://doi.org/10.1016/S0306-2619\(02\)00135-6](https://doi.org/10.1016/S0306-2619(02)00135-6).
- [4] M. Prussi, N. Scarlat, M. Acciaro, V. Kosmas, Potential and limiting factors in the use of alternative fuels in the European maritime sector, J. Clean. Prod. 291 (2021) 125849, <https://doi.org/10.1016/j.jclepro.2021.125849>.
- [5] IEA, Energy Technology Perspectives 2020. Rep., Int. Energy Agency Paris., https://scholar.google.com/scholar?hl=it&as_sdt=0%2C5&q=IEA%2C+Energy+Technology+Perspectives+2020&btnG= (Accessed May 11, 2023).
- [6] I. Singh, A.C. Tiwari, A revisit to different techniques for gas turbine blade cooling, Mater. Today Proc. (2023), <https://doi.org/10.1016/J.MATPR.2023.01.217>.
- [7] K. Mondal, L. Nuñez, C.M. Downey, L.J. van Rooyen, Recent advances in the thermal barrier coatings for extreme environments, Mater. Sci. Energy Technol. 4 (2021) 208–210, <https://doi.org/10.1016/J.MSET.2021.06.006>.
- [8] G. Gudivada, A.K. Pandey, Recent developments in nickel-based superalloys for gas turbine applications: review, J. Alloys Compd. 963 (2023) 171128, <https://doi.org/10.1016/J.JALLCOM.2023.171128>.
- [9] Y. Liu, X. Sun, V. Sethi, D. Nalianda, Y.G. Li, L. Wang, Review of modern low emissions combustion technologies for aero gas turbine engines, Prog. Aerospace Sci. 94 (2017) 12–45, <https://doi.org/10.1016/J.PAEROSCI.2017.08.001>.
- [10] H.M. Kwon, S.W. Moon, T.S. Kim, D.W. Kang, Performance enhancement of the gas turbine combined cycle by simultaneous reheating, recuperation, and coolant inter-cooling, Energy 207 (2020) 118271, <https://doi.org/10.1016/J.ENERGY.2020.118271>.
- [11] A.M. Bassily, Performance improvements of the intercooled reheat regenerative gas turbine cycles using indirect evaporative cooling of the inlet air and evaporative cooling of the compressor discharge, http://Dx.Doi.Org/10.1243/0957650011538794_215 (2001) 545–557, <https://doi.org/10.1243/0957650011538794>.
- [12] T.K. Ibrahim, M.M. Rahman, Optimum performance improvements of the combined cycle based on an intercooler-reheated gas turbine, J. Energy Resour. Technol. Trans. ASME 137 (2015), <https://doi.org/10.1115/1.4030447/372980>.
- [13] E. Global, Micro Gas Turbine Technology: Research and Development European Collaboration, 2017.
- [14] W. de Paepe, M.M. Carrero, A. Pappa, L. Briceux, F. Contino, Humidified micro gas turbine for range extended electric vehicles: thermodynamic performance assessment, Proc. ASME Turbo Expo 3 (2019), <https://doi.org/10.1115/GT2019-91389>.
- [15] H. Kim, C. Nutakor, S. Singh, A. Jaatinen-Väri, J. Nerg, J. Pyrhönen, J. Sopanen, Design process and simulations for the rotor system of a high-efficiency 22 kW micro-gas-turbine range extender for electric vehicles, Mech. Mach. Theory 183 (2023) 105230, <https://doi.org/10.1016/J.MECHMACHTHEORY.2023.105230>.
- [16] A.A. Barakat, J.H. Diab, N.S. Badawi, W.S. Bou Nader, C.J. Mansour, Combined cycle gas turbine system optimization for extended range electric vehicles, Energy Convers. Manag. 226 (2020) 113538, <https://doi.org/10.1016/J.ENCNMAN.2020.113538>.
- [17] W.S. Bou Nader, C.J. Mansour, M.G. Nemer, Optimization of a Brayton external combustion gas-turbine system for extended range electric vehicles, Energy 150 (2018) 745–758, <https://doi.org/10.1016/J.ENERGY.2018.03.008>.
- [18] F. Ji, X. Zhang, F. Du, S. Ding, Y. Zhao, Z. Xu, Y. Wang, Y. Zhou, Experimental and numerical investigation on micro gas turbine as a range extender for electric vehicle, Appl. Therm. Eng. 173 (2020) 115236, <https://doi.org/10.1016/J.APPLTHERMALENG.2020.115236>.
- [19] A. Karvountzis-Kontakiotis, A.M. Andwari, A. Pesyridis, S. Russo, R. Tuccillo, V. Esfahanian, Application of micro gas turbine in range-extended electric vehicles, Energy 147 (2018) 351–361, <https://doi.org/10.1016/J.ENERGY.2018.01.051>.
- [20] G.B. Ariemma, G. Sorrentino, R. Ragucci, M. de Joannon, P. Sabia, Ammonia/Methane combustion: stability and NOx emissions, Combust. Flame 241 (2022) 112071, <https://doi.org/10.1016/j.combustflame.2022.112071>.
- [21] G.B. Ariemma, P. Sabia, G. Sorrentino, P. Bozza, M. de Joannon, R. Ragucci, Influence of water addition on MILD ammonia combustion performances and emissions, in: Proceedings of the Combustion Institute, Elsevier Ltd, 2021: pp. 5147–5154, <https://doi.org/10.1016/j.proci.2020.06.143>.
- [22] A. Cavaliere, M. De Joannon, Mild combustion, Prog. Energy Combust. Sci. 30 (2004) 329–366, <https://doi.org/10.1016/j.pecs.2004.02.003>.
- [23] P. Sabia, G. Sorrentino, G.B. Ariemma, M.V. Manna, R. Ragucci, M. de Joannon, MILD combustion and biofuels: a minireview, Energy Fuels 35 (2021) 19901–19919, <https://doi.org/10.1021/acs.energyfuels.1c02973>.
- [24] M. de Joannon, G. Sorrentino, A. Cavaliere, MILD combustion in diffusion-controlled regimes of Hot Diluted Fuel, Combust. Flame 159 (2012) 1832–1839, <https://doi.org/10.1016/j.combustflame.2012.01.013>.
- [25] I.B. Ozdemir, N. Peters, Characteristics of the reaction zone in a combustor operating at mild combustion, Exp. Fluids 30 (2001) 683–695.
- [26] M. Derudi, R. Rota, 110th anniversary: MILD combustion of liquid hydrocarbon-alcohol blends, Ind. Eng. Chem. Res. 58 (2019) 15061–15068, <https://doi.org/10.1021/acs.iecr.9b02374>.
- [27] P. Sabia, G. Sorrentino, P. Bozza, G. Ceriello, R. Ragucci, M. De Joannon, Fuel and thermal load flexibility of a MILD burner, Proc. Combust. Inst. 37 (2019) 4547–4554, <https://doi.org/10.1016/j.proci.2018.09.003>.
- [28] L. Zheng, J. Cronly, E. Ubogu, I. Ahmed, Y. Zhang, B. Khandelwal, Experimental investigation on alternative fuel combustion performance using a gas turbine combustor, Appl. Energy 238 (2019) 1530–1542, <https://doi.org/10.1016/J.APENERGY.2019.01.175>.
- [29] B.B. Skabelund, E.B. Stechel, R.J. Milcarek, Thermodynamic analysis of a gas turbine utilizing ternary CH₄/H₂/NH₃ fuel blends, Energy 282 (2023) 128818, <https://doi.org/10.1016/J.ENERGY.2023.128818>.
- [30] T. Li, Y. Duan, Y. Wang, M. Zhou, L. Duan, Research progress of ammonia combustion toward low carbon energy, Fuel Process. Technol. 248 (2023) 107821, <https://doi.org/10.1016/J.FUPRO.2023.107821>.
- [31] A. Reine, W. Bou Nader, Fuel consumption potential of different external combustion gas-turbine thermodynamic configurations for extended range electric

- vehicles, *Energy* 175 (2019) 900–913, <https://doi.org/10.1016/J.ENERGY.2019.03.076>.
- [32] G.B. Ariemma, P. Bozza, M. De Joannon, P. Sabia, G. Sorrentino, R. Ragucci, Alcohols as energy carriers in MILD Combustion, *Energy Fuels* 35 (2021) 7253–7264, <https://doi.org/10.1021/acs.energyfuels.0c03862>.
- [33] G.B. Ariemma, G. Sorrentino, M. de Joannon, P. Sabia, A. Albano, R. Ragucci, Optical sensing for MILD Combustion monitoring, *Fuel* 339 (2023) 127479, <https://doi.org/10.1016/J.FUEL.2023.127479>.
- [34] F. Van den Schoor, R.T.E. Hermanns, J.A. van Oijen, F. Verplaetsen, L.P.H. de Goey, Comparison and evaluation of methods for the determination of flammability limits, applied to methane/hydrogen/air mixtures, *J. Hazard. Mater.* 150 (2008) 573–581, <https://doi.org/10.1016/J.JHAZMAT.2007.05.006>.
- [35] ANSYS, CHEMKIN-PRO 15131, 2013.
- [36] G.B. Ariemma, G. Sorrentino, P. Sabia, M. De Joannon, R. Ragucci, Optimization of a cyclonic combustion chamber for the thermochemical conversion of alternative fuels, *Chem. Eng. Trans.* 86 (2021) 751–756, <https://doi.org/10.3303/CET2186126>.
- [37] A. Cavaliere, M. De Joannon, R. Ragucci, Highly preheated lean combustion. *Lean Combustion*, Academic Press, 2008 www.floxxcom.ippt.gov.pl.
- [38] G. Sorrentino, A. Cavaliere, P. Sabia, R. Ragucci, M. de Joannon, Diffusion ignition processes in MILD combustion: a mini-review, *Front. Mech. Eng.* 6 (2020), <https://doi.org/10.3389/fmech.2020.00010>.
- [39] Y. Minamoto, N. Swaminathan, Subgrid scale modelling for MILD combustion, *Proc. Combust. Inst.* 35 (2015) 3529–3536. <https://doi.org/10.1016/j.proci.2014.07.025>.
- [40] G. Sorrentino, P. Sabia, M. De Joannon, A. Cavaliere, R. Ragucci, The effect of diluent on the sustainability of MILD combustion in a cyclonic burner, *Flow Turbul. Combust.* 96 (2016) 449–468, <https://doi.org/10.1007/s10494-015-9668-3>.
- [41] L. Giuntini, L. Frascino, G.B. Ariemma, C. Galletti, G. Sorrentino, R. Ragucci, Performance assessment of modeling approaches for moderate or intense low-oxygen dilution combustion in a scale-bridging burner, *Energy Fuels* (2023), <https://doi.org/10.1021/ACS.ENERGYFUELS.3C00597/ASSET/IMAGES/LARGE/EF3C00597.0011.JPEG>.
- [42] R.A.Y. Sinnott, Heat-transfer equipment, in: *Chemical Engineering Design*, third ed., Elsevier, 2014, pp. 634–793.
- [43] CRECK Modeling, C1-C3 HT+NOx mechanism.